Update on Axisymmetric VDE Benchmarking

C. R. Sovinec,[1] I. Krebs,[2] and F. J. Artola[3]

[1]*University of Wisconsin-Madison*

[2]*Dutch Institute for Fundamental Energy Research*

[3]*ITER Organization*

7th Annual Theory and Simulation of Disruptions Workshop

August 5-7, 2019 Princeton, New Jersey

Center for Tokamak Transient Simulation

Our motivation is to compare codes and models that can be used for VDE studies.

- NIMROD, M3D-C1, and JOREK are being applied to 2D and 3D disruption applications.
- Each has been verified for analytical results and with code comparisons on other applications.
- Comparisons reported here provide verification information on a realistic nonlinear VDE application.
- Isabel Krebs is coordinating the effort and reported initial results at last year's TSDW and IAEA.[1]

[1]"Axisymmetric simulations of vertical displacement events in tokamaks: A benchmark of M3D-C1, NIMROD, and JOREK," I. Krebs, *et al.* is being posted on arXiv.org and will be submitted to Physics of Plasmas.

The benchmark is based on an NSTX discharge that allowed vertical instability.

- Discharge #139536 had feedback partially turned off during the shot.
- Benchmark computations use a simplified wall shape.
- Isabel re-solved the EFIT fit from 309 ms using the M3D-C1 mesh and expansion.
- The M3D-C1 equilibrium was re-solved for NIMROD with its mesh & expansion.
- Some computations use modified Spitzer resistivity profiles: $\eta = \eta_0 \left(T - T_{off} \right)^{-3/2}$

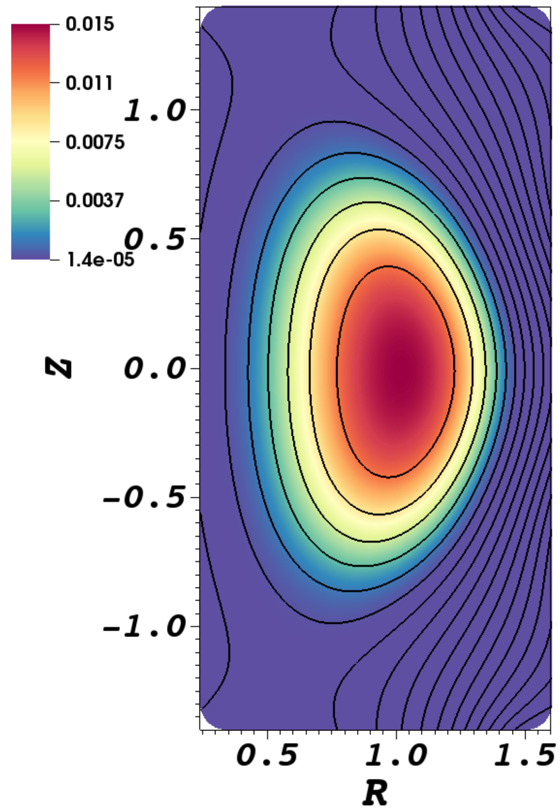

Equilibrium $\mu_0 P$ and Ψ.

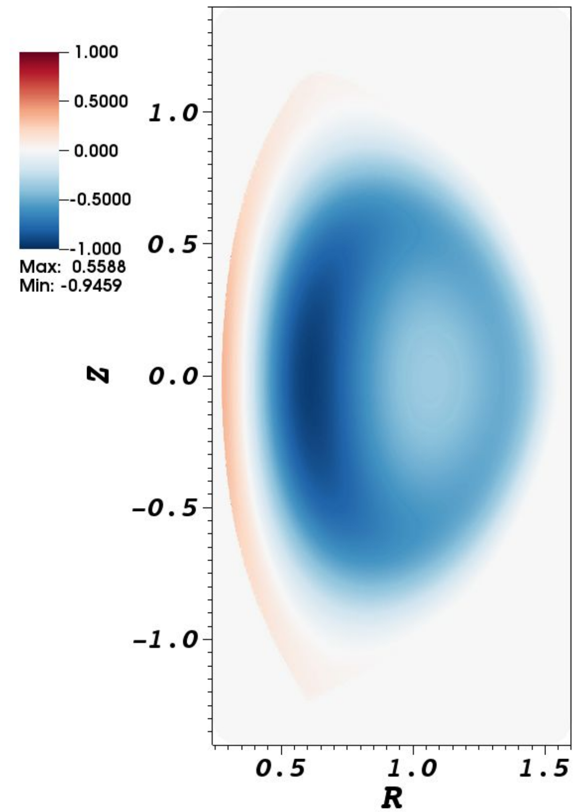

Equilibrium $\mu_0 J_\phi / R$. Note edge current layer.

Unlike JOREK, NIMROD and M3D-C1 use meshed numerical computations of external vacuum-field response.

- NIMROD couples inner and outer regions via the thin-wall model.
- M3D-C1 meshes across the resistive wall.
- JOREK couples to the STARWALL code (no outer conducting wall).

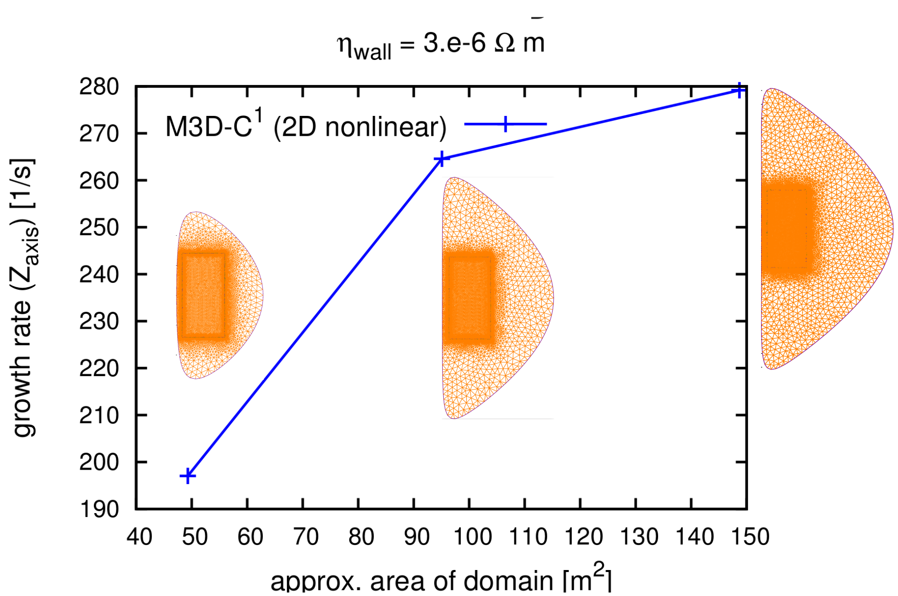

Krebs evaluated dependence on the vacuum region size.

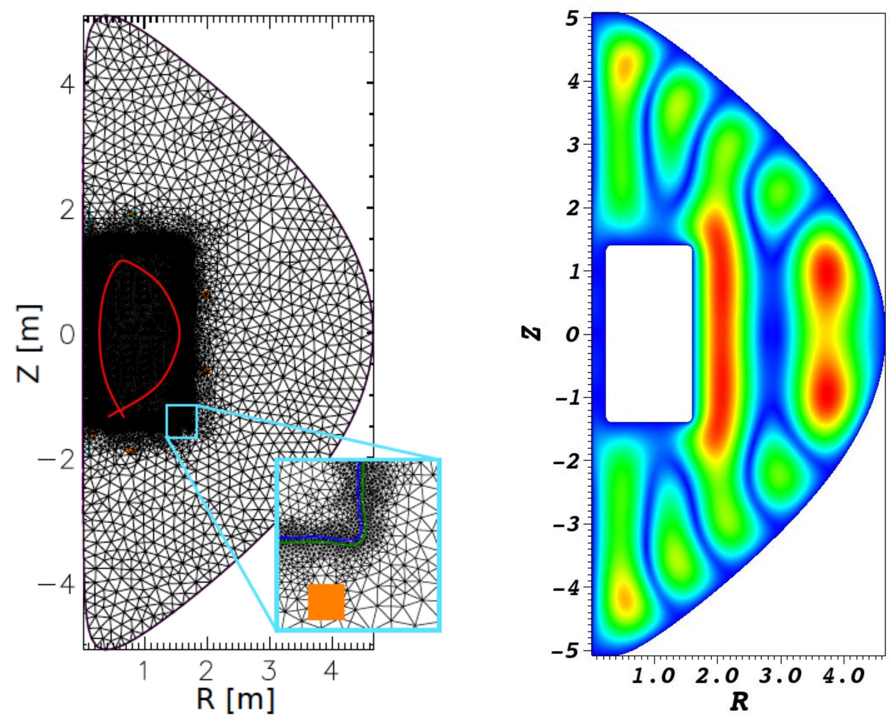

New NIMROD outer region (right – test waves plotted) is nearly the same as M3D-C1's (left).

The three codes differ in their models and in their numerical methods.

	NIMROD	M3D-C1	JOREK
MHD model	full	full	reduced used here
Linear/ nonlinear	both	both	nonlinear only (for n=0)
Poloidal representation	nodal spectral elements	reduced quintics	Bezier cubics
Toroidal rep. (not used)	Fourier	Hermite cubics	Fourier
Temporal advance	semi-implicit/ implicit	implicit	implicit

We have performed three sets of comparisons.

1. Linear η_{wall} scan
   - NIMROD and M3D-C1
   - $\kappa_{||} = \kappa_{\perp}$ $\quad T_{off} = 0$ $\quad$ [$\eta = \eta_0 \left(T - T_{off}\right)^{-3/2}$]
2. Early-phase of nonlinear η_{wall} scan
   - All three codes
   - $T_{off} = 14$ eV
   - $\kappa_{||} = 10^5 \kappa_{\perp}$
3. Nonlinear through termination
   - All three codes
   - $\kappa_{||} = 10^5 \kappa_{\perp}$ $\quad T_{off} = 0$

The most recent linear comparison shows approximately 10% discrepancy in the growth rates.

- Any discrepancies in the numerical equilibrium profiles (including edge current density) are frozen.
- There is greater sensitivity to plasma parameters at large η_{wall}.

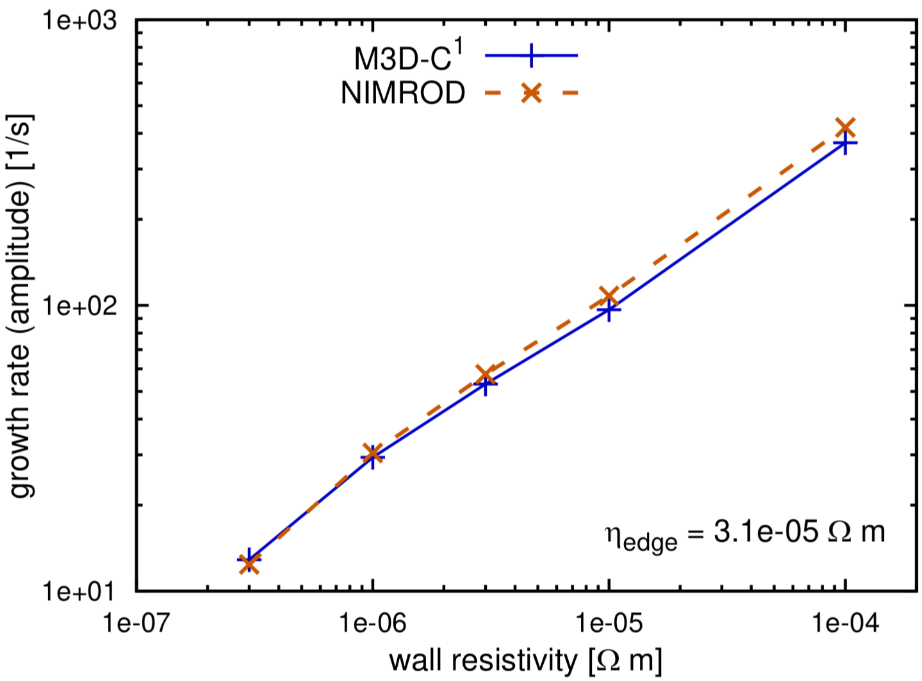

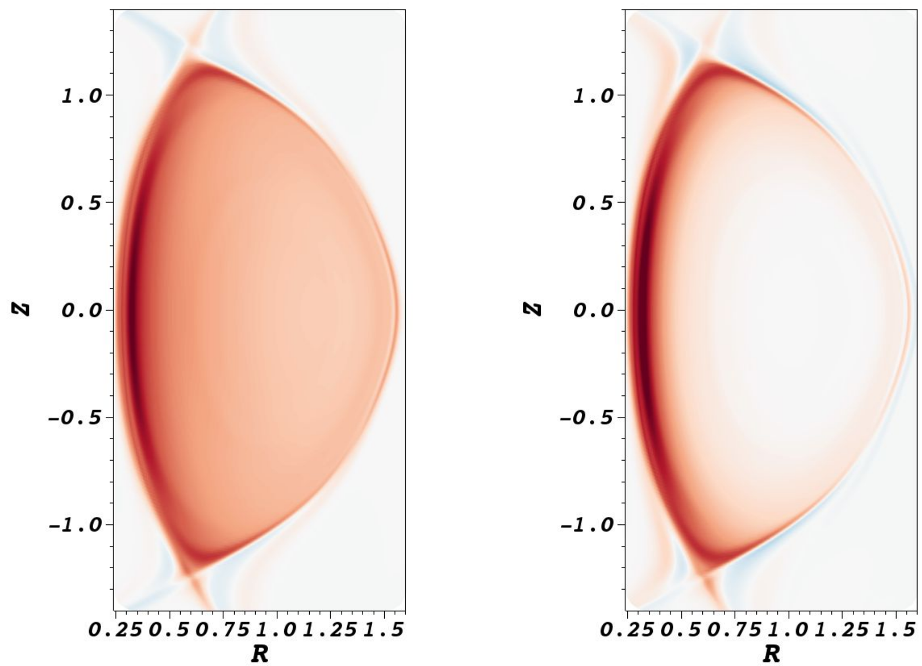

Growth-rates are within 4% at the smallest η_{wall} and within 13% at the largest η_{wall}.

V_ϕ from the smallest (left) and largest (right) η_{wall} computations from NIMROD.

A scan of η_{wall} for the early phase of nonlinear computations involves all 3 codes.

- Growth rates are inferred from fitting $Z_{axis}(t) = a + be^{-ct}$, $c \to \gamma$.
- Most values are within 12% of each other.
- Nonlinear evolution develops Pfirsch-Schlüter flows, in addition to vertical instability.

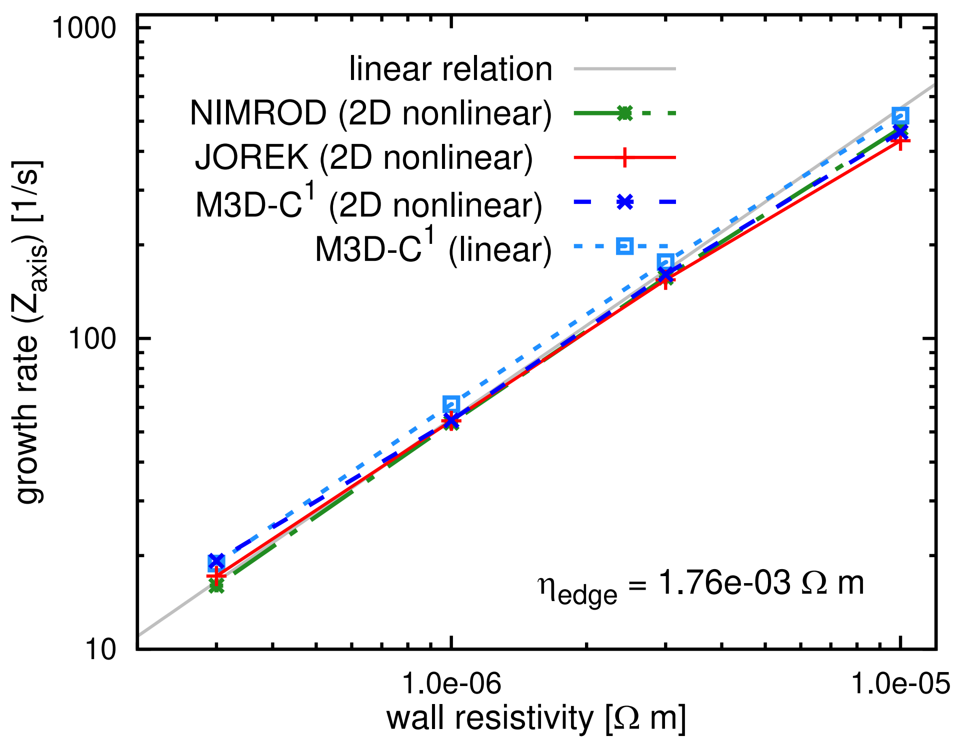

Comparison of fitted growth-rates with varied η_{wall}.

The full nonlinear computation was run though plasma termination.

- Perpendicular thermal conductivity and particle diffusivity are increased when the LCFS touches the wall.
- Output from JOREK and NIMROD are shifted in time, relative to this event.

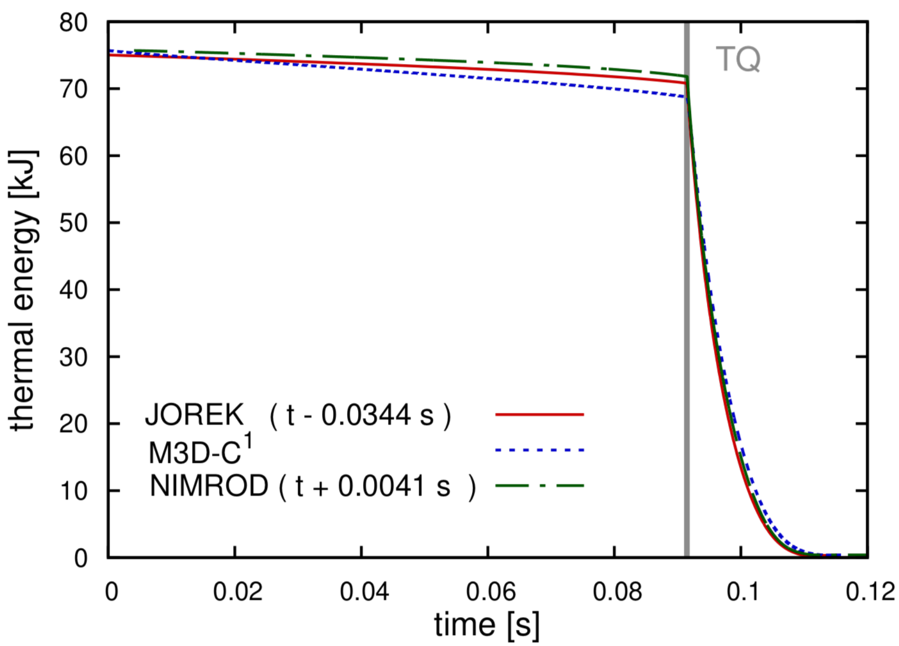

The fast thermal quench results from the increase in thermal conduction.

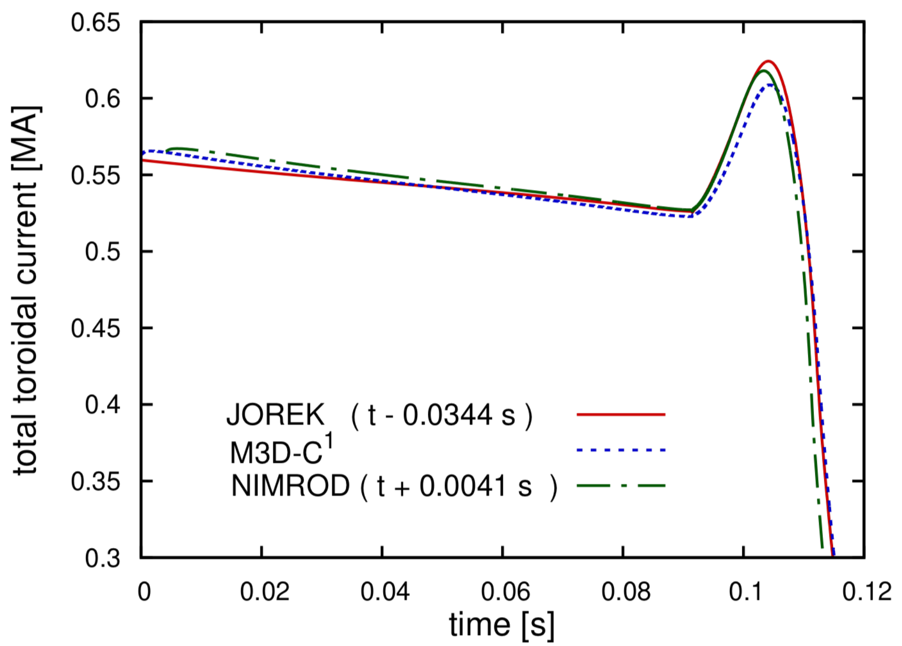

Plasma current spikes when conduction broadens the current-density distribution.

Evolution of the magnetic axis position is consistent among the three results.

- Poloidal magnetic flux is evolved in the systems of equations solved by M3D-C1 and JOREK.
- For NIMROD, poloidal flux and the magnetic axis position are generated through post-processing.

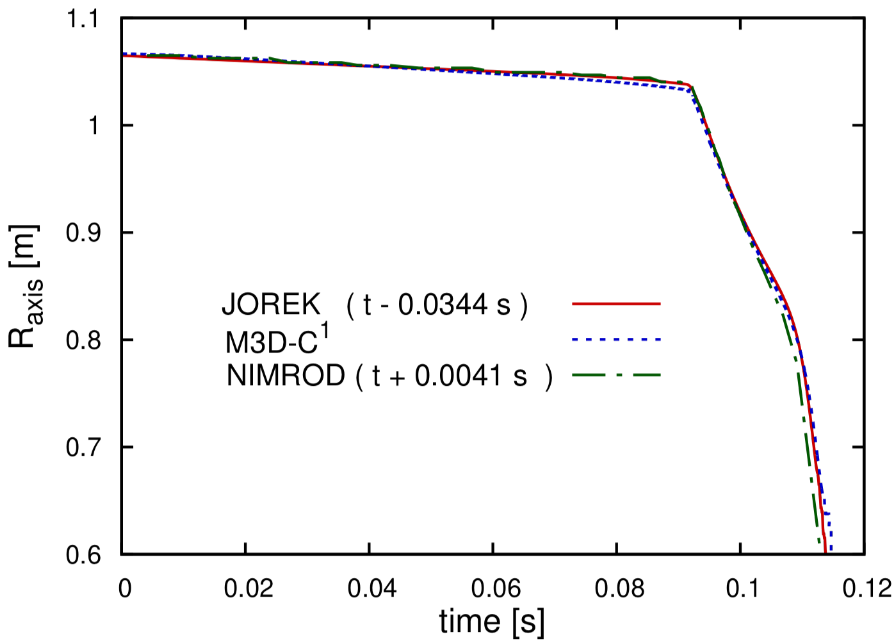

Evolution of radial position of magnetic axis.

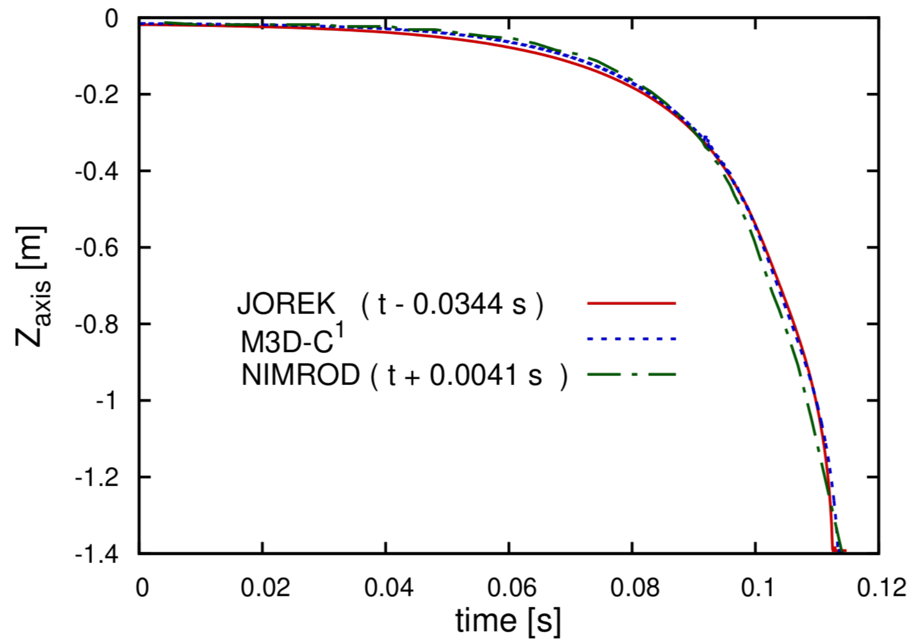

Evolution of axial position of magnetic axis.

The late-time distributions of *J*-normal agree reasonably well.

- The JOREK reduced-MHD edge $\mathbf{J}_{\mathrm{pol}} = J_{\mathrm{tor}}\mathbf{B}_{\mathrm{pol}}/B_{\mathrm{tor}}$.
- Locations and magnitudes of current density concentration are consistent.

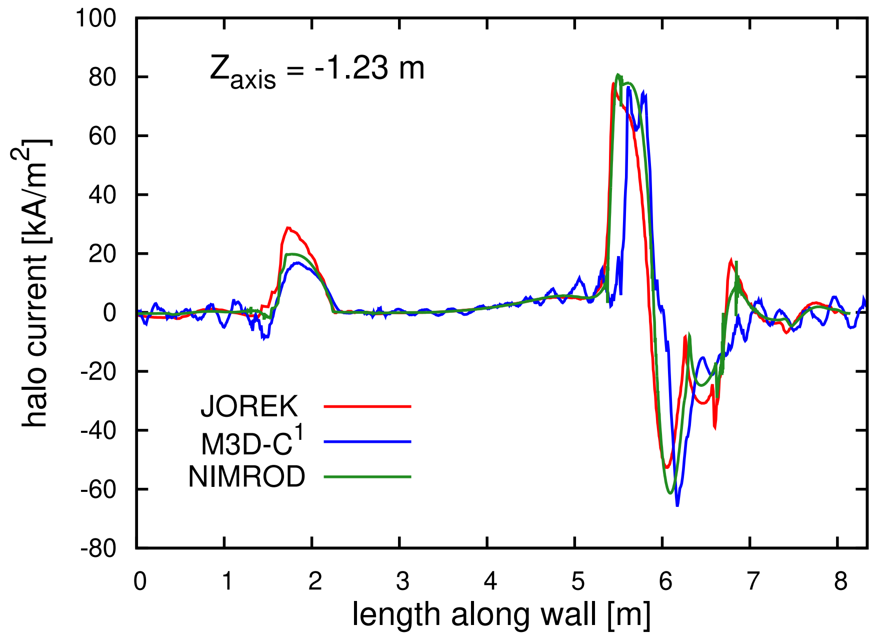

***J*-normal (halo) vs. position along wall, measured counter-clockwise.**

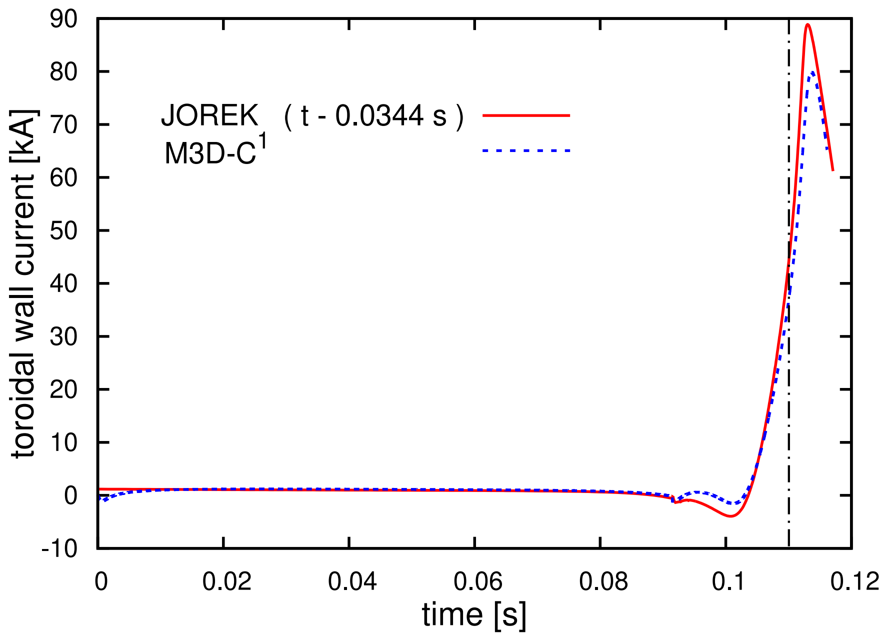

I_{wall} vs. *t* has been extracted for M3D-C1 and JOREK. Vertical line is time of *J*-normal plot.

Plot of J_{pol} (right) indicates where halo current enters and exits central region.

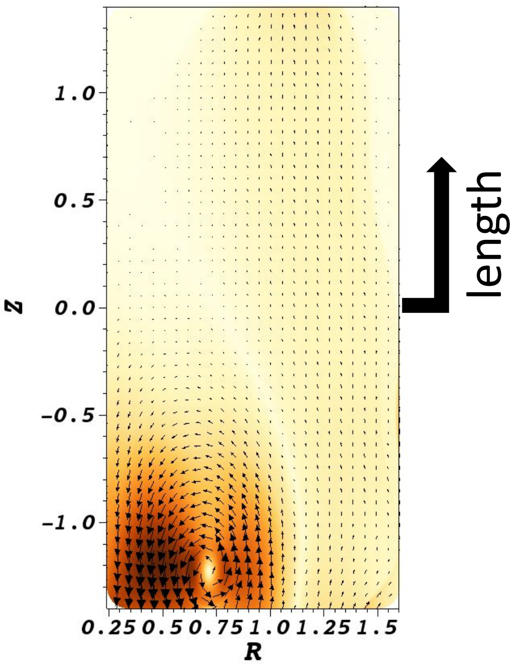

Conclusions

- For nearly all aspects, quantitative agreement is within approximately 10%.
  - M3D-C1 and NIMROD linear growth rates
  - Early nonlinear axis motion (~ all three)
    - NIMROD run for smallest η_{wall} is being continued.
  - Nonlinear current increase (all three)
  - Maximum *J*-normal from halo current (all three)
- Axisymmetric reduced-MHD reproduces the results of the full-MHD computations well.
  - Initial RB_ϕ only varies by 5%, despite small R/a.
  - Computation with the reduced system is fastest.

Discussion

- Benchmarking on realistic cases is important for critical issues like VDEs, disruption mitigation, etc.
- Benchmarking can be time-consuming.
  - Unexpected details can matter, e.g. curve-fit tolerances.
  - Understanding discrepancies involves trial and error.
  - New computational diagnostics may need to be implemented.
  - Modeling improvements are the reward.
- Recommendation: discuss as many details as possible right away (equilibrium, equations, etc.).
- Our next step is to benchmark asymmetric VDE evolution.

Extra Material

M3D-C1 and NIMROD solve full-MHD equations.

- M3D-C1 solves the equations in potential form.
- NIMROD solves them in primitive form.

$$\frac{\partial n}{\partial t} + \nabla \cdot (n\mathbf{V}) = \nabla \cdot (D \nabla n)$$

$$\rho \left(\frac{\partial}{\partial t}\mathbf{V} + \mathbf{V} \cdot \nabla \mathbf{V} \right) = \mathbf{J} \times \mathbf{B} - \nabla p - \nabla \cdot \mathbf{\Pi}$$

$$\frac{3}{2} n \left(\frac{\partial}{\partial t} T + \mathbf{V} \cdot \nabla T \right) = -\frac{p}{2} \nabla \cdot \mathbf{V} + \nabla \cdot \left[\left(\kappa_{||} - \kappa_{\perp} \right) \hat{\mathbf{b}}\hat{\mathbf{b}} + \kappa_{\perp} \mathbf{I} \right] \cdot \nabla T - T \nabla \cdot (D \nabla n)$$

$$\frac{\partial}{\partial t}\mathbf{B} = \nabla \times (\mathbf{V} \times \mathbf{B} - \eta \mathbf{J})$$

- The particle-diffusivity energy correction was added to NIMROD during the benchmarking.
- NIMROD's simplest thermal conduction typically uses constant diffusivity values and not constant conductivities.
    - A variant was developed to match M3D for benchmarking.

JOREK is used to solve the reduced-MHD equations.

$$\frac{\partial \rho}{\partial t} + \nabla \cdot (\rho \mathbf{V}) = \nabla \cdot (D \nabla_{\perp} \rho)$$

$$\widehat{\boldsymbol{\phi}} \cdot \nabla \times \left(\rho \frac{\partial}{\partial t} \mathbf{V} + \rho \mathbf{V} \cdot \nabla \mathbf{V} \right) = \widehat{\boldsymbol{\phi}} \cdot \nabla \times (\mathbf{J} \times \mathbf{B} - \nabla p + \mu \nabla^2 \mathbf{V})$$

$$\mathbf{B} \cdot \left(\rho \frac{\partial}{\partial t} \mathbf{V} + \rho \mathbf{V} \cdot \nabla \mathbf{V} \right) = \mathbf{B} \cdot (\mathbf{J} \times \mathbf{B} - \nabla p + \mu \nabla^2 \mathbf{V})$$

$$\frac{\partial}{\partial t} p + \mathbf{V} \cdot \nabla p = -\gamma p \nabla \cdot \mathbf{V} + (\gamma - 1) \nabla \cdot \left[\kappa_{||} \nabla_{||} + \kappa_{\perp} \nabla_{\perp} \right] \left(\frac{p}{\rho} \right)$$

$$\frac{1}{R^2} \frac{\partial \psi}{\partial t} = \eta \nabla \cdot \left(\frac{1}{R^2} \nabla_{\perp} \psi \right) - \mathbf{B} \cdot \nabla u$$

- See Huysmans, *et al.*, PPCF **51**, 124012 (2009).
- The variable *u* above is the streamfunction for $\mathbf{V}_{\perp}$.